Antisymmetry-breaking-coupling–enhanced sensing of quantum reservoirs

Ji-Bing Yuan [1,*] Zhi-Min Tang,[1] Ya-Ju Song,[1] Shi-Qing Tang,[1] Zhao-Hui Peng,[2] Xin-Wen Wang,[1,†] and Le-Man Kuang[3,4,‡]

[1]*Key Laboratory of Opto-electronic Control and Detection Technology of University of Hunan Province,*
and College of Physics and Electronic Engineering, Hengyang Normal University, Hengyang 421002, China

[2]*Hunan Provincial Key Laboratory of Intelligent Sensors and Advanced Sensor Materials, and Department of Physics,*
Hunan University of Science and Technology, Xiangtan 411201, China

[3]*Key Laboratory of Low-Dimensional Quantum Structures and Quantum Control of Ministry of Education,*
and Department of Physics, Hunan Normal University, Changsha 410081, China

[4]*Synergetic Innovation Academy for Quantum Science and Technology, Zhengzhou University of Light Industry, Zhengzhou 450002, China*

We investigate the use of a single generalized dephasing qubit for sensing a quantum reservoir, where the antisymmetry of the coupling between the qubit and its reservoir is broken. Our results indicate that, in addition to the decay factor encoding channel, the antisymmetry breaking coupling introduces another phase factor encoding channel. We propose an optimal measurement strategy for the generalized dephasing qubit, which enables the practical measurement precision to reach the theoretical ultimate precision quantified by the quantum signal-to-noise ratio (QSNR). As an application example, the generalized dephasing qubit is employed to estimate the *s*-wave scattering length of an atomic Bose-Einstein condensate. It is found that the QSNR contributed by the antisymmetry breaking coupling is at least two orders of magnitude higher than the QSNR contributed by the antisymmetry coupling at the millisecond timescale, and the optimal relative error can achieve a scaling $\propto 1/(\chi t)$ in long-term encoding, where χ represents the relative driving strength and t is the encoding time. Our work opens a way for supersensitive sensing of quantum reservoirs.

I. INTRODUCTION

Any realistic quantum system inevitably interacts with its surrounding quantum reservoirs, leading to quantum decoherence [1]. It is crucial to assess and characterize the quantum reservoirs for both theoretical research and practical applications such as quantum coherence protection [2,3] and reservoir engineering [4,5]. However, for a complex quantum reservoir with a large number of degrees of freedom, it is challenging to precisely estimate various parameters that characterize the quantum reservoir. An effective way to overcome the challenge is the use of quantum probes [6–15]. A quantum probe is a small and controllable quantum system prepared in a proper initial state. When the quantum probe interacts with the target quantum reservoir, quantum correlations between them will be generated. These correlations may make the probe sensitive to the reservoir's fluctuations which are induced by small changes in the parameter to be estimated. Therefore, information about the parameter may be extracted by performing an appropriate measurement on the probe. In fact, the precision of this estimation has been extensively studied using tools from the quantum parameter estimation theory [16,17]. According to the theory, the ultimate precision of any estimation procedure is limited by the

quantum Cramér-Rao (QCR) bound, which can be quantified by quantum Fisher information (QFI) or the corresponding dimensionless quantum signal-to-noise ratio (QSNR) [18,19]. A larger QFI (QSNR) indicates a higher potential achievable precision.

A single qubit (a two-level system) is the most straightforward quantum probe for estimating parameters of a quantum reservoir, attracting much attention in recent research [20–28]. If there is no energy exchange between the qubit and its reservoir, namely, the Hamiltonian of the qubit commutes with the interaction Hamiltonian between the qubit and its reservoir, the dynamical behavior of the qubit can be described by the pure dephasing model [1,29]. The pure dephasing model, which is exactly solvable, has been widely applied to detect various properties of reservoirs such as measuring ultralow temperatures [30–34], probing the cutoff frequency of Ohmic reservoirs [35–39], estimating various coupling strengthes [38–40], and detecting the non-Markovian properties [41–43]. The interaction Hamiltonian in the dephasing model of a single qubit is usually taken to be [1]

$$\hat{H}_I = \hat{\sigma}_z \sum_{\mathbf{k}} (g_{\mathbf{k}} \hat{b}_{\mathbf{k}}^\dagger + g_{\mathbf{k}}^* \hat{b}_{\mathbf{k}}), \tag{1}$$

where $\hat{\sigma}_z = |1\rangle\langle 1| - |0\rangle\langle 0|$ is the Pauli operator with $|1\rangle$ ($|0\rangle$) being the upper (lower) energy level of the qubit probe, $\hat{b}_{\mathbf{k}}(\hat{b}_{\mathbf{k}}^\dagger)$ represents the bosonic annihilation (creation) operator for the kth reservoir mode, and $g_{\mathbf{k}}$ is the coupling strength. It should be stressed that the coupling form in Eq. (1) has antisymmetry, meaning that the qubit in the lower energy level $|0\rangle$ has an

*Contact author: jbyuan@hynu.edu.cn
†Contact author: xwwang@hynu.edu.cn
‡Contact author: lmkuang@hunnu.edu.cn

opposite coupling strength with each mode of the reservoir as compared to the qubit in the upper energy level $|1\rangle$. We notice that this antisymmetry coupling (AC) only allows the reservoir's parameter information to be encoded into the qubit's decay factor, resulting in a degradation of sensing precision over time during extended encoding [44].

In this paper, we aim to fully utilize the potential of a single dephasing qubit in estimating the parameters of a quantum reservoir. To achieve this, we break the antisymmetry of the coupling in Eq. (1) and assume that the qubit in each energy level couples to each mode of the reservoir in arbitrary coupling strength. During the encoding process, we find that, in addition to the decay factor encoding channel, this antisymmetry breaking coupling (ABC) leads to the reservoir's parameters information being encoded into the qubit's phase factor. As a result, the QFI for a certain reservoir's parameter in the generalized dephasing model is composed of two parts: one part is the AC-contributed QFI, and the other part is the ABC-contributed QFI. This implies that ABC may improve the estimation precision of a single dephasing qubit for estimating reservoir's parameters. Furthermore, we propose a practical measurement scheme that enables the sensitivity of the generalized dephasing qubit to saturate the QCR bound.

To demonstrate the benefits of employing a generalized dephasing qubit for sensing quantum reservoirs, we propose a system comprising an impurity qubit immersed in an atomic Bose-Einstein condensate (BEC) to simulate the generalized dephasing model. We utilize the dephasing qubit to estimate the s-wave scattering length of the BEC, which is a crucial parameter in ultracold gases [45]. To independently quantify the sensing precision irrespective of its values, we employ the dimensionless QSNR instead of QFI for consideration. We investigate the dynamical behaviors of the AC-contributed QSNR and the ABC-contributed QSNR separately. Our findings reveal that the ABC-contributed QSNR is at least two orders of magnitude higher than the AC-contributed QSNR at the millisecond timescale. Moreover, the optimal relative error can achieve a scaling $\propto 1/(\chi t)$ in long-term encoding, indicating that ABC allows the relative driving strength (RDS) χ and the encoding time t to be utilized as resources for enhancing the sensing precision. Consequently, one can conclude that ABC makes it possible to achieve supersensitive sensing of quantum reservoirs.

II. GENERALIZED DEPHASING MODEL

The Hamiltonian of the generalized dephasing model in this paper is given as

$$\hat{H} = \frac{\omega_0}{2}\hat{\sigma}_z + \sum_{\mathbf{k}} \omega_{\mathbf{k}}\hat{b}_{\mathbf{k}}^{\dagger}\hat{b}_{\mathbf{k}} + \sum_{i=0,1}|i\rangle\langle i|\sum_{\mathbf{k}}(g_{\mathbf{k}i}\hat{b}_{\mathbf{k}}^{\dagger}+g_{\mathbf{k}i}^{*}\hat{b}_{\mathbf{k}}),$$

$$(2)$$

where ω_0 is level splitting and $\omega_{\mathbf{k}}$ is the frequency of the kth reservoir mode. The third term on the right side of the above equation is the interaction Hamiltonian, where $g_{\mathbf{k}0(1)}$ is the coupling strength between the qubit in state $|0\rangle$ ($|1\rangle$) and the kth reservoir mode. Hereafter we set $\hbar = 1$.

Using the relations $|1\rangle\langle 1| = (I + \hat{\sigma}_z)/2$ and $|0\rangle\langle 0| = (I - \hat{\sigma}_z)/2$ and omitting the constant term, the interaction

Hamiltonian

$$\hat{H}_I = \sum_{i=0,1}|i\rangle\langle i|\sum_{\mathbf{k}}(g_{\mathbf{k}i}\hat{b}_{\mathbf{k}}^{\dagger}+g_{\mathbf{k}i}^{*}\hat{b}_{\mathbf{k}}) \qquad (3)$$

is rewritten as

$$\hat{H}_I = \hat{\sigma}_z\sum_{\mathbf{k}}(g_{\mathbf{k}}\hat{b}_{\mathbf{k}}^{\dagger}+g_{\mathbf{k}}^{*}\hat{b}_{\mathbf{k}}) + \sum_{\mathbf{k}}(\xi_{\mathbf{k}}\hat{b}_{\mathbf{k}}^{\dagger}+\xi_{\mathbf{k}}^{*}\hat{b}_{\mathbf{k}}), \qquad (4)$$

where $g_{\mathbf{k}}$ is coupling strength between the Pauli operator $\hat{\sigma}_z$ of the qubit and the kth reservoir mode and the second term is effective driving term for the harmonic oscillator modes with $\xi_{\mathbf{k}}$ being the driving strength of the kth reservoir mode. There exist following relationships between $g_{\mathbf{k}}$, $\xi_{\mathbf{k}}$, $g_{\mathbf{k}0}$, and $g_{\mathbf{k}1}$:

$$g_{\mathbf{k}} = \frac{g_{\mathbf{k}1}-g_{\mathbf{k}0}}{2}, \qquad (5a)$$

$$\xi_{\mathbf{k}} = \frac{g_{\mathbf{k}1}+g_{\mathbf{k}0}}{2}. \qquad (5b)$$

It is clearly observed from Eq. (5b) that setting $g_{\mathbf{k}0} = -g_{\mathbf{k}1}$ for all modes will cause the interaction Hamiltonian (4) to degenerate into the interaction Hamiltonian (1). In this paper, the coupling of the qubit in the lower energy level having an opposite coupling strength with each mode of the reservoir as compared to the qubit in the upper energy level, i.e., $g_{\mathbf{k}0} = -g_{\mathbf{k}1}$ is referred to as AC. In the generalized depasing model we consider, the antisymmetry is broken ($g_{\mathbf{k}0} \neq -g_{\mathbf{k}1}$), resulting in the extra effective driving term in Eq. (4).

Next, we investigate how the quantum state of the qubit evolves over time under the generalized dephasing model. The initial state of the whole system is assumed to be a product state

$$\hat{\rho}_{tot}(0) = \hat{\rho}_s(0) \otimes \hat{\rho}_B(0), \qquad (6)$$

where $\hat{\rho}_s(0) = |\psi\rangle\langle\psi|$ with $|\psi\rangle = 1/\sqrt{2}(|0\rangle+|1\rangle)$ being a pure state of the probe and $\hat{\rho}_B(0) = \prod_{\mathbf{k}}(1-e^{-\beta\omega_{\mathbf{k}}})e^{-\beta\omega_{\mathbf{k}}\hat{b}_{\mathbf{k}}^{\dagger}\hat{b}_{\mathbf{k}}}$ is a thermal state of the reservoir, where $\beta = 1/k_B T$ with T and k_B being the temperature and the Boltzmann constant. Then the evolution state of the qubit probe is given as

$$\hat{\rho}_s(t) = \frac{1}{2}\begin{pmatrix} 1 & e^{-i\Phi(t)}e^{-\Gamma(t)} \\ e^{i\Phi(t)}e^{-\Gamma(t)} & 1 \end{pmatrix}, \qquad (7)$$

where the decay factor $\Gamma(t)$ is

$$\Gamma(t) = \sum_{\mathbf{k}} 4|g_{\mathbf{k}}|^2 \frac{(1-\cos\omega_{\mathbf{k}}t)}{\omega_{\mathbf{k}}^2}\coth\left(\frac{\beta\omega_{\mathbf{k}}}{2}\right), \qquad (8)$$

and the phase factor $\Phi(t)$ has the following expression:

$$\Phi(t) = \omega_0 t - \sum_{\mathbf{k}} 4\mathrm{Re}\left[\frac{\xi_{\mathbf{k}}g_{\mathbf{k}}^*}{\omega_{\mathbf{k}}}\right]t$$
$$+ \sum_{\mathbf{k}} 4\mathrm{Im}\left[\frac{\xi_{\mathbf{k}}g_{\mathbf{k}}^*}{\omega_{\mathbf{k}}^2}\left(1-e^{-i\omega_{\mathbf{k}}t}\right)\right]. \qquad (9)$$

The derivation of the time-dependent state $\hat{\rho}_s(t)$, as given in Eq. (7), is provided in detail in Appendix A. In the generalized dephasing model, the reservoir's parameter information can be encoded both in the decay factor (8) and in the phase factor (9). However, for the dephasing model with AC which is commonly employed in the study of quantum sensing of reservoirs, only the decay factor encodes reservoir parameters

due to the absence of an effective driving term ($\xi_{\mathbf{k}} = 0$). The ABC in the generalized dephasing model introduces an additional phase factor encoding channel.

III. OPTIMAL MEASUREMENT FOR THE GENERALIZED DEPHASING MODEL

In the quantum parameter estimation theory, the estimation precision of a parameter λ of interest is restricted to the QCR bound

$$\delta\lambda \geqslant \frac{1}{\sqrt{\nu \mathcal{F}_\lambda^Q}}, \tag{10}$$

where $\delta\lambda$ is the mean square error, ν represents the number of repeated experiments, and $\mathcal{F}_\lambda^Q$ denotes QFI with respect to the parameter λ. The QFI represents theoretically ultimate precision for single measurement, which can be obtained from the quantum state of the system, and more specifically, from its eigenvalues and eigenvectors. Any qubit state in the Bloch sphere representation can be written as $\hat\rho = 1/2(\hat{I} + \mathbf{w} \cdot \hat\sigma)$, where $\hat{I}$ is 2×2 identity matrix, $\mathbf{w} = (w_x, w_y, w_z)^T$ is the real Bloch vector, and $\hat\sigma = (\hat\sigma_x, \hat\sigma_y, \hat\sigma_z)$ represents the Pauli matrices. The eigenvalues of the density operator ρ can be given as $(1 \pm w)/2$, where w is the length of the Bloch vector. The length $w = 1$ for the pure state and $w < 1$ for the mixed state. In the Bloch sphere representation the QFI with respect to the estimated parameter λ can be given as follows [18,19]:

$$\mathcal{F}_\lambda^Q = \begin{cases} |\partial_\lambda \mathbf{w}|^2, & w = 1, \\ |\partial_\lambda \mathbf{w}|^2 + \frac{(\mathbf{w} \cdot \partial_\lambda \mathbf{w})^2}{1 - w^2}, & w < 1, \end{cases} \tag{11}$$

where ∂_λ denotes the derivative with respect to the estimated parameter λ. Therefore, to obtain the QFI of the evolution state $\hat\rho_S(t)$ in Eq. (7), the Bloch vector of $\hat\rho_S(t)$ is given as

$$\mathbf{w} = (\cos\Phi e^{-\Gamma}, \sin\Phi e^{-\Gamma}, 0), \tag{12}$$

with the length $w = e^{-\Gamma}$. By substituting the Bloch vector in Eq. (12) into the Eq. (11), the concrete expression of the QFI of the evolution state in Eq. (7) is obtained

$$\mathcal{F}_\lambda^Q = \frac{(\partial_\lambda \Gamma)^2}{e^{2\Gamma} - 1} + e^{-2\Gamma}(\partial_\lambda \Phi)^2. \tag{13}$$

The QFI (13) contains of two terms. The first term is the QFI of the pure dephasing model with AC, which has been extensively studied [31–35]. Therefore, we can say that the QFI of the second term is contributed by the ABC. In this paper, the first term is called AC-contributed QFI labeled as

$$\mathcal{F}_\lambda^{\parallel} = \frac{(\partial_\lambda \Gamma)^2}{e^{2\Gamma} - 1}, \tag{14}$$

and the second term is called ABC-contributed QFI denoted as

$$\mathcal{F}_\lambda^{\perp} = e^{-2\Gamma}(\partial_\lambda \Phi)^2. \tag{15}$$

Now we introduce an optimal measurement scheme for the generalized dephasing model, which enables the sensitivity of the qubit sensor to saturate the QCR bound. For a two-level system, the Fisher information associated with the measurement can be presented as [30]

$$\mathcal{F}_\lambda = \frac{1}{\langle \Delta \hat{X}^2 \rangle} \left(\frac{\partial \langle \hat{X} \rangle}{\partial \lambda} \right)^2, \tag{16}$$

where $\langle \hat{X} \rangle$ and $\langle \Delta \hat{X}^2 \rangle$ are the mean and variance of the measured observable. For an unbiased estimator, the error obeys $\delta\lambda \geqslant 1/\sqrt{\nu \mathcal{F}_\lambda} \geqslant 1/\sqrt{\nu \mathcal{F}_\lambda^Q}$, which indicates the QFI is the upper bound of the Fisher information associated with the measurement $\hat{X}$, i.e.,

$$\mathcal{F}_\lambda^Q = \max_{\hat{X}} \mathcal{F}_\lambda(\hat{X}) = \mathcal{F}_\lambda(\hat\Lambda), \tag{17}$$

with $\hat\Lambda$ being the optimal measurement. Finding the optimal measurement $\hat\Lambda$ to spur practical precision to reach the theoretically ultimate precision is of particular importance and challenge in quantum metrology. For this reason, we introduce a measurement with an measurement angle θ

$$\hat{X}_\theta = \cos\theta \hat\sigma_x + \sin\theta \hat\sigma_y, \tag{18}$$

where the angle θ is chosen by the measurer. Then the Fisher information associated with the measurement $\hat{X}_\theta$ reads

$$\mathcal{F}_\lambda(\hat{X}_\theta) = \frac{[(\partial_\lambda \Phi)\sin(\theta - \Phi) - (\partial_\lambda \Gamma)\cos(\theta - \Phi)]^2}{e^{2\Gamma} - \cos^2(\theta - \Phi)}. \tag{19}$$

It is found that when the angle θ is chosen to be the phase factor Φ, the Fisher information is equal to the AC-contributed QFI $\mathcal{F}_\lambda^{\parallel}$, and when the angle θ is chosen to be $\Phi + \pi/2$, the Fisher information is equal to the ABC-contributed QFI $\mathcal{F}_\lambda^{\perp}$, i.e.,

$$\mathcal{F}_\lambda(\hat{X}_{\theta=\Phi}) = \mathcal{F}_\lambda^{\parallel}, \quad \mathcal{F}_\lambda(\hat{X}_{\theta=\Phi+\frac{\pi}{2}}) = \mathcal{F}_\lambda^{\perp}. \tag{20}$$

It is further found that when the angle θ is set to be $\Phi + \varphi$, where φ satisfies the following equation:

$$\tan\varphi = \frac{(e^{-2\Gamma} - 1)\partial_\lambda \Phi}{\partial_\lambda \Gamma}, \tag{21}$$

the Fisher information is equal to the QFI

$$\mathcal{F}_\lambda(\hat{X}_{\theta=\Phi+\varphi}) = \mathcal{F}_\lambda^Q. \tag{22}$$

See Appendix B for the detailed verification process. Equation (22) demonstrates that the measurement $\hat{X}_{\theta=\Phi+\varphi}$ does become the optimal measurement Λ, which enables the sensitivity of the generalized dephasing qubit sensor to saturate the QCR bound. From Eq. (21), we see that the optimal measurement depends on the true value of the parameter. Therefore, measures require some prior information about the parameter λ, for which a larger sample is required. Meanwhile, the optimal measurement is time dependent, thus precise time control is necessary to achieve the predetermined optimal measurement precision.

IV. QUANTUM SENSING TO AN ATOMIC BOSE-EINSTEIN CONDENSATE

A. Quantum simulation of the generalized dephasing model

In this subsection we propose a system involving an impurity qubit immersed in a three-dimensional homogeneous

atomic BEC to simulate the generalized dephasing model. The qubit probe is confined in a harmonic trap $V_A(\mathbf{r}) = m_A \omega_A^2 r^2/2$ that is independent of the internal states, where m_A is the mass of the impurity and ω_A is the trap frequency. For $\omega_A \gg k_B T$, the spatial wave function of the qubit is the ground state of $V_A(\mathbf{r})$, i.e., $\varphi_A(\mathbf{r}) = \pi^{-3/4} \ell_A^{-3/2} \exp[-r^2/(2\ell_A^2)]$ with $\ell_A = \sqrt{1/(m_A \omega_A)}$. The Hamiltonian of the qubit is

$$\hat{H}_A = \frac{\Omega_A}{2} \hat{\sigma}_z, \tag{23}$$

where Ω_A is level splitting between the lower ($|0\rangle$) and upper ($|1\rangle$) energy levels. The Hamiltonian of the BEC is given as

$$\hat{H}_B = \int d\mathbf{r} \hat{\psi}^\dagger(\mathbf{r}) \left(-\frac{\hbar^2 \nabla_{\mathbf{r}}^2}{2m_B} + V(\mathbf{r}) - \mu \right) \hat{\psi}(\mathbf{r})$$
$$+ \frac{1}{2} g_B \int d\mathbf{r} \hat{\psi}^\dagger(\mathbf{r}) \hat{\psi}^\dagger(\mathbf{r}) \hat{\psi}(\mathbf{r}) \hat{\psi}(\mathbf{r}), \tag{24}$$

where $\hat{\psi}(\mathbf{r})$ and $\hat{\psi}^\dagger(\mathbf{r})$ are the field creation and annihilation operators, satisfying the bosonic commutative relations $[\hat{\psi}(\mathbf{r}), \hat{\psi}^\dagger(\mathbf{r}')] = \delta(\mathbf{r} - \mathbf{r}')$ and $[\hat{\psi}(\mathbf{r}), \hat{\psi}(\mathbf{r}')] = [\hat{\psi}^\dagger(\mathbf{r}), \hat{\psi}^\dagger(\mathbf{r}')] = 0$, μ is chemical potential, the contact interaction strength

$$g_B = \frac{4\pi a_B}{m_B}, \tag{25}$$

with a_B being the s-wave scattering length between one condensate atom and another and m_B being the mass of the condensate atom. Here we consider $V(\mathbf{r})$ is a very shallow spherical harmonic potential that the condensate can be taken as a homogeneous condensate. Then the field operator can be written as

$$\hat{\psi}(\mathbf{r}) = \sqrt{n} + \delta\hat{\psi}(\mathbf{r}), \tag{26}$$

where n is the density of the condensed part and $\delta\hat{\psi}(\mathbf{r})$ is the field operator of small noncondensed part. One can expand $\delta\hat{\psi}(\mathbf{r})$ as plane waves and perform Bogoliubov transformation

$$\delta\hat{\psi}(\mathbf{r}) = \frac{1}{\sqrt{\mathcal{V}}} \sum_{\mathbf{k}} (u_{\mathbf{k}} \hat{b}_{\mathbf{k}} - v_{\mathbf{k}} \hat{b}_{-\mathbf{k}}^\dagger) e^{i\mathbf{k}\cdot\mathbf{r}}, \tag{27}$$

where $\mathcal{V}$ is the volume of the BEC, $\hat{b}_{\mathbf{k}}(\hat{b}_{\mathbf{k}}^\dagger)$ is the bosonic annihilation (creation) operator satisfying the bosonic commutative relations. Here $u_{\mathbf{k}}$ and $v_{\mathbf{k}}$ are the Bogoliubov transformation coefficients with the forms $u_{\mathbf{k}} = 1/2(\sqrt{\omega_{\mathbf{k}}/E_{\mathbf{k}}} + \sqrt{E_{\mathbf{k}}/\omega_{\mathbf{k}}})$, $v_{\mathbf{k}} = 1/2(\sqrt{\omega_{\mathbf{k}}/E_{\mathbf{k}}} - \sqrt{E_{\mathbf{k}}/\omega_{\mathbf{k}}})$, where the kinetic energy $E_{\mathbf{k}} = k^2/(2m_B)$ and Bogoliubov excitation energy $\omega_{\mathbf{k}}$ reads

$$\omega_{\mathbf{k}} = \sqrt{E_{\mathbf{k}}^2 + 2n g_B E_{\mathbf{k}}}. \tag{28}$$

By substituting Eqs. (26) and (27) into the Hamiltonian (24) and omitting the constant term and the higher-order terms of $\delta\hat{\psi}(\mathbf{r})$, the Hamiltonian of the BEC is diagonalized as [46]

$$\hat{H}_B = \sum_{\mathbf{k}} \omega_{\mathbf{k}} \hat{b}_{\mathbf{k}}^\dagger \hat{b}_{\mathbf{k}}. \tag{29}$$

Let us consider the interaction Hamiltonian between the qubit probe and the BEC. For the qubit-BEC coupling, we assume that the qubit undergoes spin-dependent s-wave elastic

collisions with the BEC [6,7,30,42]. The qubit-BEC interaction Hamiltonian is represented as

$$\hat{H}_I = \left(\sum_{i=0,1} g_i |i\rangle\langle i| \right) \int d\mathbf{r} |\varphi_A(\mathbf{r})|^2 \hat{\psi}^\dagger(\mathbf{r}) \hat{\psi}(\mathbf{r}), \tag{30}$$

where

$$g_i = \frac{2\pi a_i}{m_{AB}} \tag{31}$$

is the coupling strength of the qubit-BEC interaction with a_i being the s-wave scattering length between one condensate atom and the impurity qubit in state $|i\rangle$ and m_{AB} being the reduced mass $m_{AB} = m_A m_B/(m_A + m_B)$. Since the interaction Hamiltonian (30) commutes with the Hamiltonian of the qubit in Eq. (23), the dynamical behavior of the qubit is described by the pure dephasing model. Substituting Eqs. (26) and (27) into the interaction Hamiltonian (30) and omitting the constant term and the second-order term of $\delta\hat{\psi}(\mathbf{r})$, we obtain

$$\hat{H}_I = \frac{\Delta}{2} \sigma_z + \sigma_z \sum_{\mathbf{k}} g_{\mathbf{k}} (\hat{b}_{\mathbf{k}} + \hat{b}_{\mathbf{k}}^\dagger) + \sum_{\mathbf{k}} \xi_{\mathbf{k}} (\hat{b}_{\mathbf{k}} + \hat{b}_{\mathbf{k}}^\dagger), \tag{32}$$

where $\Delta = n(g_1 - g_2)$, the coupling strength $g_{\mathbf{k}}$, and the driving strength $\xi_{\mathbf{k}}$ are given as

$$g_{\mathbf{k}} = \frac{\sqrt{n}(g_1 - g_0)}{\sqrt{\mathcal{V}}} \sqrt{\frac{E_{\mathbf{k}}}{\omega_{\mathbf{k}}}} e^{\frac{-k^2 \ell_A^2}{4}}, \tag{33a}$$

$$\xi_{\mathbf{k}} = \frac{\sqrt{n}(g_1 + g_0)}{\sqrt{\mathcal{V}}} \sqrt{\frac{E_{\mathbf{k}}}{\omega_{\mathbf{k}}}} e^{\frac{-k^2 \ell_A^2}{4}}. \tag{33b}$$

Let $\Omega_A + \Delta = \omega_0$, the total Hamiltonian is

$$\hat{H} = \frac{\omega_0}{2} \hat{\sigma}_z + \sum_{\mathbf{k}} \omega_{\mathbf{k}} \hat{b}_{\mathbf{k}}^\dagger \hat{b}_{\mathbf{k}} + \sigma_z \sum_{\mathbf{k}} g_{\mathbf{k}} (\hat{b}_{\mathbf{k}} + \hat{b}_{\mathbf{k}}^\dagger)$$
$$+ \sum_{\mathbf{k}} \xi_{\mathbf{k}} (\hat{b}_{\mathbf{k}} + \hat{b}_{\mathbf{k}}^\dagger), \tag{34}$$

which confirms that the proposed system successfully simulates the generalized dephasing model. In fact, the generalized dephasing model has been used to study the dephasing dynamics of an impurity qubit in an atomic BEC reservoir [7,41,42]. It is emphasized that the ratio of the driving strength $\xi_{\mathbf{k}}$ in Eq. (33b) to the coupling strength $g_{\mathbf{k}}$ in Eq. (33a) is a physical quantity that is independent of $\mathbf{k}$. We refer to this ratio as the RDS χ with following form:

$$\chi = \frac{\xi_{\mathbf{k}}}{g_{\mathbf{k}}} = \frac{a_1 + a_0}{a_1 - a_0}. \tag{35}$$

The above equation shows the RDS χ can be widely adjusted by changing the s-wave scattering lengths a_0 and a_1 via Feshbach resonance [47].

B. Estimating the s-wave scattering length a_B of the BEC

In this subsection, we will demonstrate the advantages of the generalized dephasing model in quantum sensing of quantum reservoirs. To illustrate, we employ the impurity qubit to estimate the s-wave scattering length a_B of the BEC, a crucial parameter in ultracold gases [45]. The initial state of the impurity qubit and BEC is prepared to be the state in Eq. (6). Under
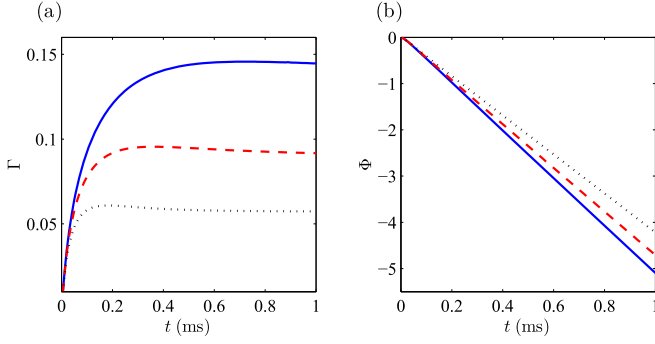
FIG. 1. Dynamical behaviors of the decay factor Γ in (a) and the phase factor Φ in (b) for the s-wave scattering lengths $a_B = 0.5a_{Rb}$ (blue solid line), $a_B = a_{Rb}$ (red dashed line), and $a_B = 2a_{Rb}$ (black dotted line). The RDS is taken as $\chi = 1$.

the control of the Hamiltonian (34), the evolution state of the impurity qubit must be the state in Eq. (7). Substituting $g_{\mathbf{k}}$ in Eq. (33a) and $\xi_{\mathbf{k}}$ in Eq. (33b) into the decay factor in Eq. (8) and the phase factor in Eq. (9), then using the continuum limit $\sum_{\mathbf{k}} \to \frac{\mathcal{V}}{(2\pi)^3} \int_0^{2\pi} d\varphi \int_0^{\pi} \sin\theta d\theta \int_0^{\infty} k^2 dk$, we obtain the decay factor

$$\Gamma(t) = P \int_0^{\infty} k^2 \frac{E_{\mathbf{k}}(1 - \cos\omega_{\mathbf{k}}t)}{\omega_{\mathbf{k}}^3} e^{\frac{-k^2\ell_A^2}{2}} dk, \qquad (36)$$

and the phase factor

$$\Phi(t) = \chi P \int_0^{\infty} k^2 \frac{E_{\mathbf{k}}(\sin\omega_{\mathbf{k}}t - \omega_{\mathbf{k}}t)}{\omega_{\mathbf{k}}^3} e^{\frac{-k^2\ell_A^2}{2}} dk, \qquad (37)$$

where we consider the zero temperature reservoir and the parameter $P = 2n(g_1 - g_0)^2/\pi^2$.

We present numerical results based on Eqs. (36) and (37) after determining reasonable parameter values. We consider a ^{23}Na impurity atom is immersed in a ^{87}Rb BEC with density $n = 10^{20}$ m^{-3}. The impurity atom is trapped in an optical lattice with trapped characteristic length $\ell_A = 45$ nm. The difference between the spin-dependent s-wave scattering lengths is taken to be $a_1 - a_0 = 2.9$ nm. The s-wave scattering length a_B of the BEC is restricted by the condition $\sqrt{na_B^3} \ll 1$. As a consequence, the scattering length has to satisfy the inequality $a_B < 3a_{Rb}$, where $a_{Rb} = 5.3$ nm [41,48].

The dynamical behaviors of the decay factor Γ and the phase factor Φ for different s-wave scattering lengths $a_B = 0.5a_{Rb}$ (blue solid line), $a_B = a_{Rb}$ (red dashed line), and $a_B = 2a_{Rb}$ (black dotted line) are depicted in Figs. 1(a) and 1(b), respectively. The decay factors for the three s-wave scattering lengths increase with time from zero and eventually reach different stationary values and the phase factors decrease with time, as shown in Figs. 1(a) and 1(b). Moreover, the decay factor differences caused by changing a_B tend to stabilize over time, but the phase factor differences caused by changing a_B become larger with time. The stationary value $\Gamma(\infty)$ for the s-wave scattering length $a_B = 0.5a_{Rb}$ is 0.14, the off-diagonal element $\rho_{10}(t)$ of the density matrix $\hat{\rho}_s(t)$ in Eq. (7) will maintain a stable nonzero value $|\rho_{10}(\infty)| = 1/2e^{-\Gamma(\infty)} = 0.43$. This means that the quantum coherence of the qubit in the BEC reservoir can be preserved at $|\rho_{10}(\infty)|/|\rho_{10}(0)| =$

87%. We can see that increasing s-wave scattering length is beneficial for preserving quantum coherence. The preservation of quantum coherence of a qubit in the BEC reservoir was addressed in previous studies [7,41,48]. Now we introduce the spectral density function to understand the phenomenon of maintaining quantum coherence. The spectral density function is defined as $J(\omega) = \sum_{\mathbf{k}} 4|g_{\mathbf{k}}|^2 \delta(\omega - \omega_{\mathbf{k}})$. Then the decay factor in Eq. (36) can be rewritten as

$$\Gamma(t) = \int_0^{\infty} J(\omega) \frac{1 - \cos\omega t}{\omega^2} d\omega. \qquad (38)$$

It is known that the dynamical behavior of the decay factor $\Gamma(t)$ depends on the specific form of the spectral density function $J(\omega)$ [1]. For example, when the spectral density function is a super-Ohmic spectrum, i.e., $J(\omega) \propto \omega^s$ with $s > 1$, the decay factor will approach a finite positive value over time, leading to the phenomenon of coherence preservation in dephasing qubits [29,38]. In our proposed system, according to the coupling strength $g_{\mathbf{k}}$ in Eq. (33a), the spectral density function is given as

$$J(\omega) = Q \frac{k(\omega)^4}{\omega} \left(\frac{d\omega}{dk}\Big|_{k=k(\omega)} \right)^{-1} e^{-\frac{1}{2}\ell_A^2 k(\omega)^2}, \qquad (39)$$

where the parameter $Q = n(g_1 - g_2)^2/(\pi^2 m_B)$ and $k(\omega)$ is obtained from the following dispersion relation:

$$\omega \equiv \omega_{\mathbf{k}} = \frac{k\sqrt{k^2 + 16\pi na_B}}{2m_B}. \qquad (40)$$

Different from Ohmic-family spectrum which is phenomenologically given, the specific form of this spectral density in Eq. (39) depends on the dispersion relation of the BEC in Eq. (40), and is independent of the ABC. For example, when the wave vector $k \ll 4\sqrt{\pi na_B}$, the dispersion relation is that of a phonon $\omega = c_s k$ with the velocity of sound $c_s = 2\sqrt{\pi na_B}/m_B$. In this case, with $k(\omega) = \omega/c_s$, the spectral density function can be approximated as a super-Ohmic spectrum $J(\omega) \propto \omega^3$. In short, the structure of the spectral density function, as determined by the dispersion relation of the BEC, leads to the phenomenon of maintaining quantum coherence.

To quantify the sensing precision of the s-wave scattering length a_B independently of its values, we introduce the dimensionless QSNR

$$Q_{a_B} = a_B^2 \mathcal{F}_{a_B}^Q, \qquad (41)$$

along with the AC-contributed QSNR $Q_{a_B}^{\parallel} = a_B^2 \mathcal{F}_{a_B}^{\parallel}$ and the ABC-contributed QSNR $Q_{a_B}^{\perp} = a_B^2 \mathcal{F}_{a_B}^{\perp}$. From the QCR bound in Eq. (10), the optimal relative error and the QSNR has the relation

$$\frac{(\delta a_B)_{\min}}{a_B} = \frac{1}{\sqrt{\nu Q_{a_B}}}, \qquad (42)$$

which indicates the QSNR quantifies the ultimate precision of quantum sensing. Figures 2(a) and 2(b) plot the dynamical behaviors of the AC-contributed QSNR $Q_{a_B}^{\parallel}$ and the ABC-contributed QSNR $Q_{a_B}^{\perp}$ for different s-wave scattering lengths $a_B = 0.5a_{Rb}$ (blue solid line), $a_B = a_{Rb}$ (red dashed line), and $a_B = 2a_{Rb}$ (black dotted line). All AC-contributed QSNRs in Fig. 2(a) increase from zero to different steady values with time, while all ABC-contributed QSNRs in Fig. 2(b) increase
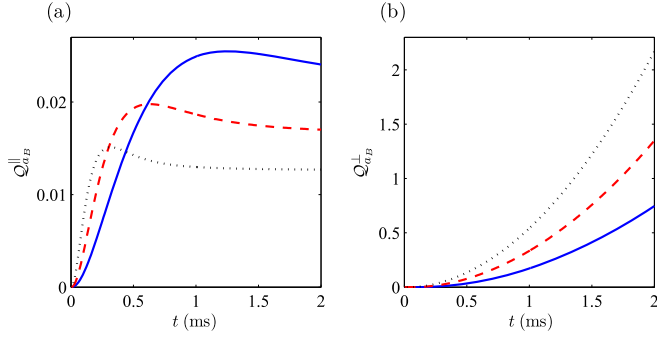
FIG. 2. Time dependence of the AC-contributed QSNR $Q_{a_B}^{\parallel}$ in (a) and the ABC-contributed QSNR $Q_{a_B}^{\perp}$ in (b) for the *s*-wave scattering lengths $a_B = 0.5a_{Rb}$ (blue solid line), $a_B = a_{Rb}$ (red dashed line), and $a_B = 2a_{Rb}$ (black dotted line). The RDS is taken as $\chi = 1$.

continuously over time. In particular, it is observed that at the millisecond timescale, the ABC-contributed QSNR is at least two orders of magnitude higher than the AC-contributed QSNR for the same *s*-wave scattering length a_B. This demonstrates that the phase factor encoding channel caused by the ABC greatly enhances the ultimate precision of quantum sensing for the *s*-wave scattering length a_B. We also need to emphasize that the dynamical behaviors where the QSNR $Q_{a_B}^{\parallel}$ remains unchanged over time and the QSNR $Q_{a_B}^{\perp}$ increases with time both require the preservation of quantum coherence in the qubit.

To further explore the relationship of the ABC-contributed QSNR $Q_{a_B}^{\perp}$ with the encoding time t and the RDS χ, we define such a ratio

$$\eta = \frac{Q_{a_B}^{\perp}}{(\chi t)^2}. \tag{43}$$

The dynamical behaviors of the ratio η in Eq. (43) are presented in Fig. 3 for different *s*-wave scattering lengths $a_B = 0.5a_{Rb}$ (blue solid line), $a_B = a_{Rb}$ (red dashed line), and $a_B = 2a_{Rb}$ (black dotted line). As observed, all ratios increase with time to distinct stable values, with the ratio corresponding to a smaller *s*-wave scattering length a_B exhibiting a smaller
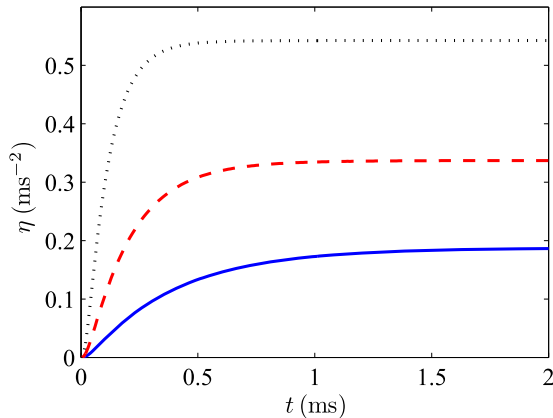

FIG. 3. The ratio η as a function of time t for the *s*-wave scattering lengths $a_B = 0.5a_{Rb}$ (blue solid line), $a_B = a_{Rb}$ (red dashed line), and $a_B = 2a_{Rb}$ (black dotted line).
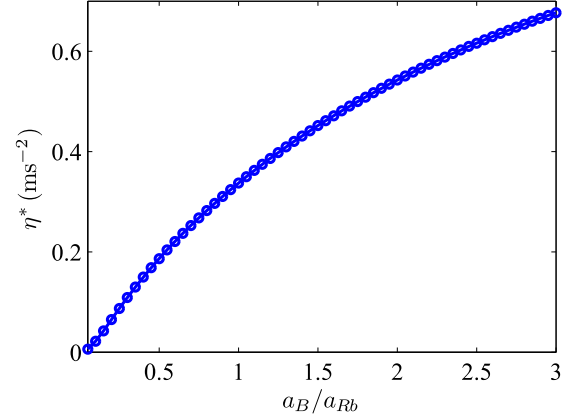

FIG. 4. The optimal ratio η^* as a function of the dimensionless *s*-wave scattering length of the BEC a_B/a_{Rb}.

stable value. In fact, such similar dynamical behaviors are still presented for other *s*-wave scattering lengths. This implies that there exists an optimal ratio η^* that is independent of the encoding time t and positively correlated with the *s*-wave scattering length a_B in long-term encoding. The relationship between the optimal ratio η^* and the dimensionless *s*-wave scattering length a_B/a_{Rb} is depicted in Fig. 4, which shows that η^* increases as a_B increases.

In long-term encoding, due to $Q_{a_B}^{\perp} \gg Q_{a_B}^{\parallel}$, the QSNR Q_{a_B} can be approximated as

$$Q_{a_B} \approx Q_{a_B}^{\perp} = \eta^*(\chi t)^2, \tag{44}$$

thus the optimal relative error has following simple expression:

$$\frac{(\delta a_B)_{min}}{a_B} = \frac{1}{\sqrt{\nu \eta^*} \chi t}. \tag{45}$$

Equation (45) illustrates that encoding time t serves as a resource to augment the ultimate precision of quantum sensing for the *s*-wave scattering length a_B. Additionally, it demonstrates that increasing the RDS χ in Eq. (35) can also enhance the ultimate precision.

Finally, considering the complexity of the optimal measurement to better demonstrate the superiority of ABC in parameter estimation, we investigate the ratio of the Fisher information associated with the measurement $\hat{\sigma}_x$ for the pure dephasing model with ABC to the one for the pure dephasing model with AC

$$\mathcal{R} = \frac{\mathcal{F}_{a_B}(\hat{\sigma}_x)}{\mathcal{F}_{a_B}^{\parallel}}, \tag{46}$$

where $\mathcal{F}_{a_B}(\hat{\sigma}_x)$ is given as

$$\mathcal{F}_{a_B}(\hat{\sigma}_x) = \frac{[\cos\Phi(\partial_{a_B}\Gamma) + \sin\Phi(\partial_{a_B}\Phi)]^2}{e^{2\Gamma} - \cos^2\Phi}. \tag{47}$$

Here it should be noted that, for the pure dephasing model with AC, the AC-contributed QFI $\mathcal{F}_{a_B}^{\parallel}$ is equivalent to the Fisher information associated with the measurement $\hat{\sigma}_x$ [31–35]. The ratio $\mathcal{R} > 1$ means that the ABC can enhance the precision of estimating a_B through the measurement $\hat{\sigma}_x$, and the larger the value of $\mathcal{R}$, the more significant the effect of enhancing precision. Figure 5 shows the dynamic behavior
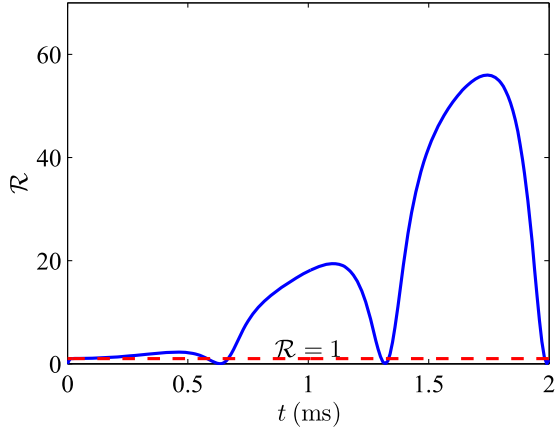
FIG. 5. The ratio $\mathcal{R}$ as a function of time t for the s-wave scattering lengths $a_B = a_{Rb}$.

of the ratio $\mathcal{R}$ oscillating over time, which is attributed to the presence of trigonometric functions involving the time-dependent phase factor Φ in the Fisher information (47). Moreover, the local peaks for each oscillation constantly increase with time, as the absolute value of $\partial_{a_B}\Phi$ in Eq. (47) grows with time. Therefore, we can conclude that the ABC can effectively enhance the precision of the s-wave scattering length estimation, attained by the measurement of $\hat{\sigma}_x$, for the majority of the time.

V. CONCLUSION

In conclusion, we studied the utilization of a single generalized dephasing qubit for sensing of a quantum reservoir. In the generalized dephasing model, the antisymmetry of coupling between the qubit and its reservoir is broken. Our findings revealed that, in addition to the decay factor encoding channel, the ABC introduces another encoding channel, namely, the phase factor encoding channel. We employed the QFI to quantify the ultimate precision of quantum sensing and discovered that the QFI associated with the generalized dephasing qubit consists of the AC-contributed QFI and the ABC-contributed QFI. Furthermore, we proposed an optimal measurement scheme for the generalized dephasing qubit, which enables the practical measurement precision to reach the theoretical ultimate precision.

To demonstrate the benefits of employing a generalized dephasing qubit for quantum reservoir sensing, we proposed a system comprising an impurity qubit immersed in an atomic BEC to simulate the generalized dephasing model. We utilized the impurity qubit to estimate the s-wave scattering length of the BEC. To independently quantify the sensing precision irrespective of its values, the dimensionless QSNR instead of QFI was employed for analysis. We separately examined the dynamical behaviors of AC-contributed QSNR and ABC-contributed QSNR. Our results indicated that the ABC-contributed QSNR is at least two orders of magnitude higher than the AC-contributed QSNR at the millisecond timescale. Additionally, the ABC-contributed QSNR increases continuously with time, while the AC-contributed QSNR remains constant during long-term encoding. Notably, we discovered

that the optimal relative error can achieve a scaling $\propto 1/(\chi t)$ during extended encoding. This means that extending the encoding time t and increasing the RDS χ can enhance sensing of the s-wave scattering length of the BEC. Finally, we studied the dynamics of the ratio $\mathcal{R}$, which is defined as the Fisher information associated with the measurement $\hat{\sigma}_x$ under pure dephasing model with ABC to the one under pure dephasing model with AC. It was found that the ABC can also effectively improve the precision of the s-wave scattering length estimation, attained by the measurement of $\hat{\sigma}_x$, for the majority of the time.

The generalized dephasing model can also be well used for the sensing of other quantum reservoirs such as Ohmic-family reservoirs [35–39]. It is worth noting that the ABC enables the encoding of key parameters of the Ohmic-family spectral density, such as the cutoff frequency and reservoir coupling strength, into the phase factor of the generalized dephasing qubit. Our work opens a way for supersensitive sensing of quantum reservoirs.

APPENDIX A: DERIVATION OF EVOLUTION STATE OF THE QUBIT IN THE GENERALIZED DEPHASING MODEL

We first introduce a unitary transformation

$$\hat{U} = \exp\left[\sum_{\mathbf{k}}\left(\hat{\alpha}_{\mathbf{k}}\hat{b}_{\mathbf{k}}^\dagger - \hat{\alpha}_{\mathbf{k}}^\dagger\hat{b}_{\mathbf{k}}\right)\right] \equiv \Pi_{\mathbf{k}}\hat{U}_{\mathbf{k}}(\hat{\alpha}_{\mathbf{k}}), \quad \text{(A1)}$$

where $\hat{U}_{\mathbf{k}}(\hat{\alpha}_{\mathbf{k}}) = \exp(\hat{\alpha}_{\mathbf{k}}\hat{b}_{\mathbf{k}}^\dagger - \hat{\alpha}_{\mathbf{k}}^\dagger\hat{b}_{\mathbf{k}})$ is the kth mode unitary transformation operator with

$$\hat{\alpha}_{\mathbf{k}} = \frac{g_{\mathbf{k}}\hat{\sigma}_z + \xi_{\mathbf{k}}}{\omega_{\mathbf{k}}}. \quad \text{(A2)}$$

Using the relation $\exp(\hat{A})\hat{B}\exp(-\hat{A}) = \hat{B} + [\hat{A}, \hat{B}] + \frac{[\hat{A},[\hat{A},\hat{B}]]}{2!} + \cdots$, we obtain

$$\hat{U}_{\mathbf{k}}(\hat{\alpha}_{\mathbf{k}})\hat{b}_{\mathbf{k}}^\dagger\hat{b}_{\mathbf{k}}\hat{U}_{\mathbf{k}}^\dagger(\hat{\alpha}_{\mathbf{k}}) = \hat{b}_{\mathbf{k}}^\dagger\hat{b}_{\mathbf{k}} - \hat{\alpha}_{\mathbf{k}}\hat{b}_{\mathbf{k}}^\dagger - \hat{\alpha}_{\mathbf{k}}^\dagger\hat{b}_{\mathbf{k}} + \hat{\alpha}_{\mathbf{k}}\hat{\alpha}_{\mathbf{k}}^\dagger + \hat{\alpha}_{\mathbf{k}}^\dagger\hat{\alpha}_{\mathbf{k}}, \quad \text{(A3)}$$

$$\hat{U}_{\mathbf{k}}(\hat{\alpha}_{\mathbf{k}})(g_{\mathbf{k}}\hat{b}_{\mathbf{k}}^\dagger + g_{\mathbf{k}}^*\hat{b}_{\mathbf{k}})\hat{U}_{\mathbf{k}}^\dagger(\hat{\alpha}_{\mathbf{k}}) = (g_{\mathbf{k}}\hat{b}_{\mathbf{k}}^\dagger + g_{\mathbf{k}}^*\hat{b}_{\mathbf{k}}) - (g_{\mathbf{k}}\hat{\alpha}_{\mathbf{k}}^\dagger + g_{\mathbf{k}}^*\hat{\alpha}_{\mathbf{k}}). \quad \text{(A4)}$$

Then we perform the unitary transformation $\hat{U}$ on the Hamiltonian (2) of the main text and obtain

$$
\hat{H}' = \hat{U}\hat{H}\hat{U}^\dagger = \frac{1}{2}\omega_0\hat{\sigma}_z + \sum_{\mathbf{k}}\omega_{\mathbf{k}}\hat{b}_{\mathbf{k}}^\dagger\hat{b}_{\mathbf{k}}
$$
$$
+ \sum_{\mathbf{k}}[\omega_{\mathbf{k}}(\hat{\alpha}_{\mathbf{k}}\hat{\alpha}_{\mathbf{k}}^\dagger + \hat{\alpha}_{\mathbf{k}}^\dagger\hat{\alpha}_{\mathbf{k}}) - \hat{\sigma}_z(g_{\mathbf{k}}\hat{\alpha}_{\mathbf{k}}^\dagger + g_{\mathbf{k}}^*\hat{\alpha}_{\mathbf{k}})
$$
$$
- (\xi_{\mathbf{k}}\hat{\alpha}_{\mathbf{k}}^\dagger + \xi_{\mathbf{k}}^*\hat{\alpha}_{\mathbf{k}})]. \tag{A5}
$$

By simplifying the above equation and omitting the constant term, we obtain

$$
\hat{H}' = \frac{1}{2}\Delta\hat{\sigma}_z + \sum_{\mathbf{k}}\omega_{\mathbf{k}}\hat{b}_{\mathbf{k}}^\dagger\hat{b}_{\mathbf{k}}, \tag{A6}
$$

where

$$
\Delta = \omega_0 - \sum_{\mathbf{k}}4\mathrm{Re}\left[\frac{\xi_{\mathbf{k}}g_{\mathbf{k}}^*}{\omega_{\mathbf{k}}}\right]. \tag{A7}
$$

The evolution state of the qubit probe is represented as

$$
\hat{\rho}_s(t) = \mathrm{Tr}_B[e^{-i\hat{H}t}\hat{\rho}_s(0)\otimes\hat{\rho}_B(0)e^{i\hat{H}t}]
$$
$$
\equiv \mathrm{Tr}_B[\hat{U}^\dagger e^{-i\hat{H}'t}\hat{U}\hat{\rho}_s(0)\otimes\hat{\rho}_B(0)\hat{U}^\dagger e^{i\hat{H}'t}\hat{U}]. \tag{A8}
$$

According to the above equation, we can easily prove the diagonal elements unchanged. The off-diagonal elements are given as

$$
\rho_{s,10}(t) = \rho_{s,01}(t)^* = \langle 1|\hat{\rho}_s(t)|0\rangle = \frac{1}{2}e^{-i\Delta t}f_B(t). \tag{A9}
$$

Here $f_B(t)$ is a reservoir-dependent function with the following expression:

$$
f_B(t) = \prod_{\mathbf{k}}\mathrm{Tr}_B[\hat{D}_{\mathbf{k}}^\dagger(\alpha_{\mathbf{k},0})e^{it\omega_{\mathbf{k}}\hat{b}_{\mathbf{k}}^\dagger\hat{b}_{\mathbf{k}}}\hat{D}_{\mathbf{k}}(\alpha_{\mathbf{k},0})\hat{D}_{\mathbf{k}}^\dagger(\alpha_{\mathbf{k},1})
$$
$$
\times e^{-it\omega_{\mathbf{k}}\hat{b}_{\mathbf{k}}^\dagger\hat{b}_{\mathbf{k}}}\hat{D}_{\mathbf{k}}(\alpha_{\mathbf{k},1})\hat{\rho}_{B,\mathbf{k}}(0)], \tag{A10}
$$

where $\hat{D}_{\mathbf{k}}(\alpha_{\mathbf{k}}) = \exp(\alpha_{\mathbf{k}}\hat{b}_{\mathbf{k}}^\dagger - \alpha_{\mathbf{k}}^*\hat{b}_{\mathbf{k}})$ is the kth mode Glauber displacement operator with $\alpha_{\mathbf{k},1} = (\xi_{\mathbf{k}} + g_{\mathbf{k}})/\omega_{\mathbf{k}}$, $\alpha_{\mathbf{k},0} = (\xi_{\mathbf{k}} - g_{\mathbf{k}})/\omega_{\mathbf{k}}$ and $\hat{\rho}_{B,\mathbf{k}}(0) = (1 - e^{-\beta\omega_{\mathbf{k}}})e^{-\beta\omega_{\mathbf{k}}\hat{b}_{\mathbf{k}}^\dagger\hat{b}_{\mathbf{k}}}$ is a thermal state of the kth mode. Using the following relations:

$$
\hat{D}(\alpha)\hat{D}(\beta) = \hat{D}(\alpha + \beta)\exp[i\mathrm{Im}(\alpha\beta^*)],
$$
$$
\exp(x\hat{b}^\dagger\hat{b})\hat{D}(\alpha)\exp(-x\hat{b}^\dagger\hat{b}) = \hat{D}(\alpha e^x), \tag{A11}
$$

we obtain

$$
f_B(t) = e^{-i\Theta(t)}e^{-\Gamma(t)}, \tag{A12}
$$

where the decaying function is

$$
e^{-\Gamma(t)} = \prod_{\mathbf{k}}\mathrm{Tr}_B[\hat{D}_{\mathbf{k}}[(\alpha_{\mathbf{k},1} - \alpha_{\mathbf{k},0})(1 - e^{i\omega_{\mathbf{k}}t})]\hat{\rho}_{B,\mathbf{k}}(0)]
$$
$$
= \exp\left[-\sum_{\mathbf{k}}4|g_{\mathbf{k}}|^2\frac{(1 - \cos\omega_{\mathbf{k}}t)}{\omega_{\mathbf{k}}^2}\coth\left(\frac{\beta\omega_{\mathbf{k}}}{2}\right)\right], \tag{A13}
$$

and the phase factor is given as

$$
\Theta(t) = \sum_{\mathbf{k}}\mathrm{Im}[\alpha_{\mathbf{k},0}(\alpha_{\mathbf{k},0} - \alpha_{\mathbf{k},1})^*e^{-i\omega_{\mathbf{k}}t}
$$
$$
+ \alpha_{\mathbf{k},1}^*(\alpha_{\mathbf{k},1} - \alpha_{\mathbf{k},0})e^{i\omega_{\mathbf{k}}t} + 2\alpha_{\mathbf{k},0}\alpha_{\mathbf{k},1}^*]
$$
$$
= \sum_{\mathbf{k}}4\mathrm{Im}\left[\frac{\xi_{\mathbf{k}}g_{\mathbf{k}}^*}{\omega_{\mathbf{k}}^2}\left(1 - e^{-i\omega_{\mathbf{k}}t}\right)\right]. \tag{A14}
$$

APPENDIX B: DERIVATION OF THE FISHER INFORMATION ASSOCIATED WITH THE MEASUREMENTS

The evolution state in Eq. (7) of the main text is rewritten as

$$
\hat{\rho}_S(t) = \frac{1}{2}(I + e^{-\Gamma(t)}\cos\Phi\hat{\sigma}_x + e^{-\Gamma(t)}\sin\Phi\hat{\sigma}_y). \tag{B1}
$$

We introduce a measurement operator

$$
\hat{X}_\theta = \cos\theta\hat{\sigma}_x + \sin\theta\hat{\sigma}_y. \tag{B2}
$$

The mean and the variance of this measurement operator in quantum state (B1) are given as

$$
\langle\hat{X}_\theta\rangle = e^{-\Gamma}\cos(\theta - \Phi), \quad \left\langle\Delta\hat{X}_\theta^2\right\rangle = 1 - e^{-2\Gamma}\cos^2(\theta - \Phi). \tag{B3}
$$

Here it is important to emphasize that the angle θ is chosen by the measurer and is not a function of the parameter λ to be estimated. Then the Fisher information associated with the measurement $\hat{X}_\theta$ reads

$$
\mathcal{F}_\lambda(\hat{X}_\theta) = \frac{(\partial_\lambda\langle\hat{X}_\theta\rangle)^2}{\left\langle\Delta\hat{X}_\theta^2\right\rangle}
$$
$$
= \frac{[(\partial_\lambda\Phi)\sin(\theta - \Phi) - (\partial_\lambda\Gamma)\cos(\theta - \Phi)]^2}{e^{2\Gamma} - \cos^2(\theta - \Phi)}. \tag{B4}
$$

(i) According to the Fisher information in Eq. (B4), if one chooses the measurement angle $\theta = \Phi$, the Fisher information equals to AC-contributed QFI, i.e.,

$$
\mathcal{F}_\lambda(\hat{X}_{\theta=\Phi}) = \frac{(\partial_\lambda\Gamma)^2}{e^{2\Gamma} - 1} = \mathcal{F}_\lambda^\parallel. \tag{B5}
$$

(ii) If one chooses the measurement angle $\theta = \Phi + \pi/2$, the Fisher information equals to ABC-contributed QFI, i.e.,

$$
\mathcal{F}_\lambda(\hat{X}_{\theta=\Phi+\frac{\pi}{2}}) = e^{-2\Gamma}(\partial_\lambda\Phi)^2 = \mathcal{F}_\lambda^\perp. \tag{B6}
$$

(iii) We will look for an optimal measurement angle θ_{opt} that makes the Fisher information $\mathcal{F}_\lambda(\hat{X}_{\theta=\theta_{\mathrm{opt}}})$ equal to the QFI $\mathcal{F}_\lambda^Q$. We assume that the optimal measurement angle can be expressed as $\theta_{\mathrm{opt}} = \Phi + \varphi$. According to the Fisher information in Eq. (B4), the Fisher information $\mathcal{F}_\lambda(\hat{X}_{\theta=\Phi+\varphi})$ reads

$$
\mathcal{F}_\lambda(\hat{X}_{\theta=\Phi+\varphi}) = \frac{\sin^2\varphi(\partial_\lambda\Phi)^2 + \cos^2\varphi(\partial_\lambda\Gamma)^2 - 2\sin\varphi\cos\varphi(\partial_\lambda\Phi)(\partial_\lambda\Gamma)}{e^{2\Gamma} - \cos^2\varphi}. \tag{B7}
$$

If $\hat{X}_{\theta=\Phi+\varphi}$ is the optimal measurement $\hat{\Lambda}$, it has to satisfy $\mathcal{F}_\lambda(\hat{X}_{\theta=\Phi+\frac{\pi}{2}}) = \mathcal{F}_\lambda^Q$, i.e.,

$$\frac{\sin^2\varphi(\partial_\lambda\Phi)^2 + \cos^2\varphi(\partial_\lambda\Gamma)^2 - 2\sin\varphi\cos\varphi(\partial_\lambda\Phi)(\partial_\lambda\Gamma)}{e^{2\Gamma} - \cos^2\varphi} = \frac{(\partial_\lambda\Gamma)^2}{e^{2\Gamma} - 1} + e^{-2\Gamma}(\partial_\lambda\Phi)^2. \tag{B8}$$

By simplifying the above equation, we obtain

$$a\tan^2\varphi + b\tan\varphi + c = 0, \tag{B9}$$

where $a = (\partial_\lambda\Gamma)^2/(1 - e^{-2\Gamma})$, $b = 2(\partial_\lambda\Phi)(\partial_\lambda\Gamma)$, and $c = (1 - e^{-2\Gamma})(\partial_\lambda\Phi)^2$. By solving Eq. (B9), we obtain

$$\tan\varphi = \frac{(e^{-2\Gamma} - 1)\partial_\lambda\Phi}{\partial_\lambda\Gamma}. \tag{B10}$$

[1] H. P. Breuer and F. Petruccione, *The Theory of Open Quantum Systems* (Oxford University Press, Oxford, 2007).

[2] L. Viola, E. Knill, and S. Lloyd, Dynamical decoupling of open quantum systems, Phys. Rev. Lett. **82**, 2417 (1999).

[3] Q. S. Tan, Y. Huang, X. Yin, L. M. Kuang, and X. Wang, Enhancement of parameter estimation precision in noisy systems by dynamical decoupling pulses, Phys. Rev. A **87**, 032102 (2013).

[4] J. I. Cirac, A. S. Parkins, R. Blatt, and P. Zoller, "Dark" squeezed states of the motion of a trapped ion, Phys. Rev. Lett. **70**, 556 (1993).

[5] J. F. Poyatos, J. I. Cirac, and P. Zoller, Quantum reservoir engineering with laser cooled trapped ions, Phys. Rev. Lett. **77**, 4728 (1996).

[6] A. Recati, P. O. Fedichev, W. Zwerger, J. von Delft, and P. Zoller, Atomic quantum dots coupled to a reservoir of a superfluid Bose-Einstein condensate, Phys. Rev. Lett. **94**, 040404 (2005).

[7] M. A. Cirone, G. De Chiara, G. M. Palma, and A. Recati, Collective decoherence of cold atoms coupled to a Bose-Einstein condensate, New J. Phys. **11**, 103055 (2009).

[8] C. Benedetti, F. Buscemi, P. Bordone, and M. G. A. Paris, Quantum probes for the spectral properties of a classical environment, Phys. Rev. A **89**, 032114 (2014).

[9] M. Bina, F. Grasselli, and M. G. A. Paris, Continuous-variable quantum probes for structured environments, Phys. Rev. A **97**, 012125 (2018).

[10] M. Mehboudi, A. Lampo, C. Charalambous, L. A. Correa, M. Á. García-March, and M. Lewenstein, Using polarons for sub-nK quantum nondemolition thermometry in a Bose-Einstein condensate, Phys. Rev. Lett. **122**, 030403 (2019).

[11] D. Tamascelli, C. Benedetti, H. P. Breuer, and M. G. A. Paris, Quantum probing beyond pure dephasing, New J. Phys. **22**, 083027 (2020).

[12] W. Wu, S. Y. Bai, and J. H. An, Non-Markovian sensing of a quantum reservoir, Phys. Rev. A **103**, L010601 (2021).

[13] A. V. Kirkova, W. Li, and P. A. Ivanov, Adiabatic sensing technique for optimal temperature estimation using trapped ions, Phys. Rev. Res. **3**, 013244 (2021).

[14] D. Adam, Q. Bouton, J. Nettersheim, S. Burgardt, and A. Widera, Coherent and dephasing spectroscopy for single-impurity probing of an ultracold bath, Phys. Rev. Lett. **129**, 120404 (2022).

[15] M. M. Khan, M. Mehboudi, H. Terças, M. Lewenstein, and M. A. Garcia-March, Subnanokelvin thermometry of an interacting *d*-dimensional homogeneous Bose gas, Phys. Rev. Res. **4**, 023191 (2022).

[16] C. W. Helstrom, *Quantum Detection and Estimation Theory* (Academic, New York, 1976).

[17] A. S. Holevo, *Probabilistic and Statistical Aspects of Quantum Theory* (North-Holland, Amsterdam, 1982).

[18] W. Zhong, Z. Sun, J. Ma, X. G. Wang, and F. Nori, Fisherer information under decoherence in bloch representation, Phys. Rev. A **87**, 022337 (2013).

[19] J. Liu, H. D. Yuan, X. M. Lu, and X. G. Wang, Quantum Fisherer information matrix and multiparameter estimation, J. Phys. A: Math. Theor. **53**, 023001 (2020).

[20] Y. M. Chu, Y. Liu, H. B. Liu, and J. M. Cai, Quantum sensing with a single-qubit pseudo-Hermitian system, Phys. Rev. Lett. **124**, 020501 (2020).

[21] S. P. Wolski, D. Lachance-Quirion, Y. Tabuchi, S. Kono, A. Noguchi, K. Usami, and Y. Nakamura, Dissipation-based quantum sensing of magnons with a superconducting qubit, Phys. Rev. Lett. **125**, 117701 (2020).

[22] S. Fernandez-Lorenzo and D. Porras, Quantum sensing close to a dissipative phase transition: Symmetry breaking and criticality as metrological resources, Phys. Rev. A **96**, 013817 (2017).

[23] W. Wu and C. Shi, Quantum parameter estimation in a dissipative environment, Phys. Rev. A **102**, 032607 (2020).

[24] F. Chapeau-Blondeau, Quantum parameter estimation on coherently superposed noisy channels, Phys. Rev. A **104**, 032214 (2021).

[25] W. T. He, H. Y. Guang, Z. Y. Li, R. Q. Deng, N. N. Zhang, J. X. Zhao, F. G. Deng, and Q. Ai, Quantum metrology with one auxiliary particle in a correlated bath and its quantum simulation, Phys. Rev. A **104**, 062429 (2021).

[26] J.-H. Lü, W. Ning, X. Zhu, F. Wu, L. T. Shen, Z. B. Yang, and S. B. Zheng, Critical quantum sensing based on the Jaynes-Cummings model with a squeezing drive, Phys. Rev. A **106**, 062616 (2022).

[27] L. Xu, J. B. Yuan, S. Q. Tang, W. Wu, Q. S. Tan, and L. M. Kuang, Non-Markovian enhanced temperature sensing in a dipolar Bose-Einstein condensate, Phys. Rev. A **108**, 022608 (2023).

[28] K. Kakuyanagi, H. Toida, L. V. Abdurakhimov, and S. Saito, Submicrometer-scale temperature sensing using quantum

coherence of a superconducting qubit, New J. Phys. **25**, 013036 (2023).

[29] A. J. Leggett, S. Chakravarty, A. T. Dorsey, M. P. A. Fisher, Anupam Garg, and W. Zwerger, Dynamics of the dissipative two-state system, Rev. Mod. Phys. **59**, 1 (1987).

[30] M. T. Mitchison, T. Fogarty, G. Guarnieri, S. Campbell, T. Busch, and J. Goold, In situ thermometry of a cold fermi gas via dephasing impurities, Phys. Rev. Lett. **125**, 080402 (2020).

[31] S. Razavian, C. Benedetti, M. Bina, Y. Akbari-Kourbolagh, and M. G. A. Paris, Quantum thermometry by single-qubit dephasing, Eur. Phys. J. Plus **134**, 284 (2019).

[32] F. Gebbia, C. Benedetti, F. Benatti, R. Floreanini, M. Bina, and M. G. A. Paris, Two-qubit quantum probes for the temperature of an ohmic environment, Phys. Rev. A **101**, 032112 (2020).

[33] A. Candeloro and M. G. A. Paris, Discrimination of ohmic thermal baths by quantum dephasing probes, Phys. Rev. A **103**, 012217 (2021).

[34] J. B. Yuan, B. Zhang, Y. J. Song, S. Q. Tang, X. W. Wang, and L. M. Kuang, Quantum sensing of temperature close to absolute zero in a Bose-Einstein condensate, Phys. Rev. A **107**, 063317 (2023).

[35] C. Benedetti, F. Salari Sehdaran, M. H. Zandi, and M. G. A. Paris, Quantum probes for the cutoff frequency of ohmic environments, Phys. Rev. A **97**, 012126 (2018).

[36] F. Salari Sehdaran, M. Bina, C. Benedetti, and M. G. A. Paris, Quantum probes for ohmic environments at thermal equilibrium, Entropy **21**, 486 (2019).

[37] F. Salari Sehdaran, M. H. Zandi, and A. Bahrampour, The effect of probe-ohmic environment coupling type and probe information of the cutoff frequency, Phys. Lett. A **383**, 126006 (2019).

[38] Q. S. Tan, W. Wu, L. Xu, J. Liu, and L. M. Kuang, Quantum sensing of supersensitivity for the Ohmic quantum reservoir, Phys. Rev. A **106**, 032602 (2022).

[39] H. Ather and A. Z. Chaudhry, Improving the estimation of environment parameters via initial probe-environment correlations, Phys. Rev. A **104**, 012211 (2021).

[40] Q. S. Tan, J. B. Yuan, J. Q. Liao, and L. M. Kuang, Supersensitive estimation of the coupling rate in cavity optomechanics with an impurity-doped Bose-Einstein condensate, Opt. Express **28**, 22867 (2020).

[41] P. Haikka, S. McEndoo, G. De Chiara, G. M. Palma, and S. Maniscalco, Quantifying, characterizing, and controlling information flow in ultracold atomic gases, Phys. Rev. A **84**, 031602(R) (2011).

[42] P. Haikka, S. McEndoo, and S. Maniscalco, Non-Markovian probes in ultracold gases, Phys. Rev. A **87**, 012127 (2013).

[43] J. B. Yuan, H. J. Xing, L. M. Kuang, and S. Yi, Quantum non-Markovian reservoirs of atomic condensates engineered via dipolar interactions, Phys. Rev. A **95**, 033610 (2017).

[44] C. L. Degen, F. Reinhard, and P. Cappellaro, Quantum sensing, Rev. Mod. Phys. **89**, 035002 (2017).

[45] I. Bloch, J. Dalibard, and W. Zwerger, Many-body physics with ultracold gases, Rev. Mod. Phys. **80**, 885 (2008).

[46] D. van Oosten, P. van der Straten, and H. T. C. Stoof, Quantum phases in an optical lattice, Phys. Rev. A **63**, 053601 (2001).

[47] C. Chin, R. Grimm, P. Julienne, and E. Tiesinga, Feshbach resonances in ultracold gases, Rev. Mod. Phys. **82**, 1225 (2010).

[48] Y. J. Song and L. M. Kuang, Controlling decoherence speed limit of a single impurity atom in a Bose-Einstein-condensate reservoir, Ann. Phys. (NY) **531**, 1800423 (2019).